**RESEARCH ARTICLE**

# Assessing the environmental risk, fractions, and remobilization of copper and zinc in the sediments of the Jialing River—an important tributary of the Yangtze River in China

Tuo Zhang[1] · Lijuan Li[2] · Fei Xu[1] · Xiangyu Chen[1] · Li Du[1] · Yunxiang Li[1]

## Abstract

Copper (Cu) and zinc (Zn) are two heavy metal pollutants that pose a serious risk in the Jialing River. Cu and Zn are transported into the sediment primarily due to the activities of the mining and smelting industries. In this study, we employed the diffusive gradient in thin films (DGT) technique, sequential extraction, and two assessment methods to evaluate the remobilization, fractions, and environmental risk in the downstream section of the Jialing River. The total concentrations of Cu and Zn in the four study areas followed the order S3 > S2 > S4 > S1, and the assessment results indicated that Cu and Zn presented a low environmental risk in the study area. Cu and Zn were primarily bound to the Fe/Mn oxide fraction (F2) and the residual fraction (F4). The results of the DGT probe showed a clear vertical distribution of Cu and Zn in the sediment (from 3 to − 12 cm), and both elements showed obvious increasing trends at the bottom of the probe. The correlation analysis indicated that $C_{DGT}$-Cu correlated well with $C_{DGT}$-Zn ($r = 0.834$, $p < 0.01$). The flux results showed that the sediment in the downstream section of the Jialing River is a major source of Cu and Zn and that there is a potential risk of release to the overlying water. Further analysis found that $C_{DGT}$-Fe was negatively correlated with $C_{DGT}$-Cu and $C_{DGT}$-Zn, indicating that Fe may influence the remobilization of these metals. In addition, a hotspot of $C_{DGT}$-Cu and $C_{DGT}$-Zn at the bottom of the probe corresponded with a dark area in the AgI gel measuring $C_{DGT}$-S. These results indicate that Fe and S are factors that mitigate the release of Cu and Zn from sediments.

**Keywords** Jialing River · Sediment · Cu · Zn · DGT

## Introduction

Currently, heavy metal pollution in sediments is of great concern due to its toxicity, resistance to degradation, and tendency to bioaccumulate (Ndiba et al. 2008; Zhang et al. 2014; Yin and Zhu 2016). Heavy metals may originate from both natural processes and anthropogenic activities. Natural processes include rock and soil weathering and erosion, which are generally very slow processes and generally do not result in substantial environmental pollution (Dalman et al. 2006).

✉ Tuo Zhang
   xiaotuodujiang@126.com

[1] College of Environmental Science & Engineering, China West Normal University, Nanchong 637009, Sichuan, China

[2] Institute of Agricultural Environment and Sustainable Development, Chinese Academy of Agriculture Sciences, Beijing 100081, China

Conversely, major anthropogenic activities, such as mining, smelting, municipal wastewater treatment, and urban and agricultural runoff, can be major sources of environmental pollution (Equeenuddin et al. 2013). Sediment, as an important component of the aquatic environment, has attracted extensive attention because it can act as a considerable sink or source of heavy metals (Akcay et al. 2003; Yin and Zhu 2016). Sediments can control the transition, behavior, and availability of trace metals in aquatic environments (Islam et al. 2015; Fisher-Power et al. 2016). The adsorption affinity for trace metals typically relies on the geochemical components of sediments, such as organic matter, metal oxides (particularly Fe and Mn oxides), and clay minerals, which have been shown to be important in trace metal adsorption (Shi et al. 2013; Dang et al. 2015). If the geochemical properties of the sediment change (e.g., pH or redox potential) within the aquatic system, there is a potential environmental risk from the release of heavy metals from the solid phase into the aqueous phase, where they are more readily taken up by aquatic organisms (Simpson et al. 2000; Peng et al. 2009; Zhang et al. 2016).

Hence, as the occurrence of heavy metals in sediments is a dynamic process, it is important to find suitable approaches to study the dynamic release of heavy metals from sediment or the adsorption of heavy metals to sediments.

The diffusive gradient in thin films (DGT) technique is recognized as a robust in situ passive tool for predicting the bioavailability of metals in sediments (Zhang and Davison 1995). Unlike traditional chemical extraction methods, DGT accounts for the resupply of metals from the solid phase to the solution phase; therefore, DGT simulates the transmembrane movement of the elements and has shown a good correlation with plant uptake (Williams et al. 2009; Warnken et al. 2008). The technique samples both free and weakly bound elements, which compose the DGT-labile fraction (Buzier et al. 2014). A DGT probe can provide a large amount of information, including the vertical distribution of metals on a fine scale, the calculation of apparent fluxes, and the mechanism of the dynamic release of heavy metals from sediment. In addition, a well-established three-step sequential extraction scheme (European Community Bureau of Reference, BCR) is widely accepted as a powerful tool to differentiate the various heavy metal fractions bound in soils or sediments (Pueyo et al. 2008). The BCR scheme is a good supplement to the DGT technique and allows a complete and systemic study of heavy metal chemical behavior in sediment.

Copper (Cu) and zinc (Zn) are the two main heavy metal contaminants in the Jialing River. Industries involving the mining, smelting, and processing of non-ferrous metals have long been concentrated along the middle and upstream sections of the Jialing River. During the mining process, Cu, Zn, Pb, and Cd are released into the environment. To date, little work has been conducted to assess the environmental risk and remobilization of Cu and Zn in the downstream region of the Jialing River. Whether the downstream region of the Jialing River is affected by the mid-upstream mining industry is unknown. Thus, the aims of this study were (1) to assess the environmental risk of Cu and Zn in the downstream section of the Jialing River, (2) to understand the fractions and horizontal and vertical distributions of Cu and Zn in the sediment, and (3) to identify the factors and mechanisms that control Cu and Zn remobilization from the sediment.

## Materials and methods

### Study area and sample collection

The study area was located in the downstream section of the Jialing River (31° 07′ to 30° 05′, 106° 18′ to 106° 46′) (Fig. 1). This area includes the flow from Nanchong City (the second largest population center in Sichuan Province with over 7.5 million people) to Chongqing (a municipality of over 30 million people). Four sediment core samples were collected at Qingquan Temple (S1), Dingjia Village (S2), Litou Village (S3), and Liuwenxue Tomb (S4) along the downstream section of the Jialing River in January 2019. The four core samples were taken from positions approximately 5–10 m from the riverbank with a core sampler. The sample cores were then taken to the riverbank and vertically inserted into a soft sleeve to minimize disturbance. The sleeves were placed in a specially prepared dark Teflon box (with a constant temperature of 4 ± 1 °C and a nitrogen atmosphere), which was immediately sealed to prevent exposure to oxygen. The four cores were incubated at 25 °C for 24 h to allow equilibration after the sediment cores arrived at the laboratory.

### DGT probe preparation, deployment, and elution

The commercially available DGT probe was obtained from Weishen Environment Ltd. (Nanjing, China). The window size of the assembled DGT probe was 150 mm (length) × 18-mm (width). The DGT probe was combined with three membranes: a protective 0.45-μm cellulose-acetate filter layer, a 0.4-mm polyacrylamide gel diffusive layer, and a Chelex-100 gel layer as an adsorption sink for heavy metals. In addition, a silver iodide (AgI) diffusive gel was added to the DGT probe to measure the dissolved sulfides (Wu et al. 2015; Xu et al. 2016). The AgI diffusive gel was introduced before the Chelex-100 gel to react with sulfides to form black $Ag_2S$. The probes were stored at 4 °C until deployment in the sediment.

Deployment of the DGT probe was conducted as described by Gao et al. (2016). The DGT deployment was conducted in an incubator at 25 °C in the dark. Briefly, the DGT probes were first marked with a 3-cm water-sediment label from the top of the DGT window as the boundary to distinguish the water and sediment interface in an oxygen-free box, and the DGT probe was stored in this box for at least 24 h. The deployment of the DGT probes and storage of the sediment cores were performed in an anaerobic glovebox (96% $N_2$/4% $H_2$) to ensure that no oxygen was introduced into the sediment. The DGT probe was then carefully inserted into the sediment, and the sediment core was sealed tightly and transferred to a 25 °C incubator. After 24 h of deployment, the DGT probe was retrieved and the adsorption gel was cut into 5-mm vertical segments with a Teflon-coated blade. The slices were then transferred to 2-mL centrifuge tubes with 1 mL of a 1 M $HNO_3$ solution to elute the DGT-labile Cu, Zn, and Fe for further analysis. Then, the eluted solution was diluted ten times and was ready for measurement. The Cu, Zn, and Fe concentrations were then analyzed by inductively coupled plasma mass spectrometry (ICP-MS, Thermo Fisher Scientific, X SERIES, USA) (Motelica-Heino et al. 2003).

The mass ($M$) of the target element accumulated by the DGT sampling device was calculated with Eq. (1):
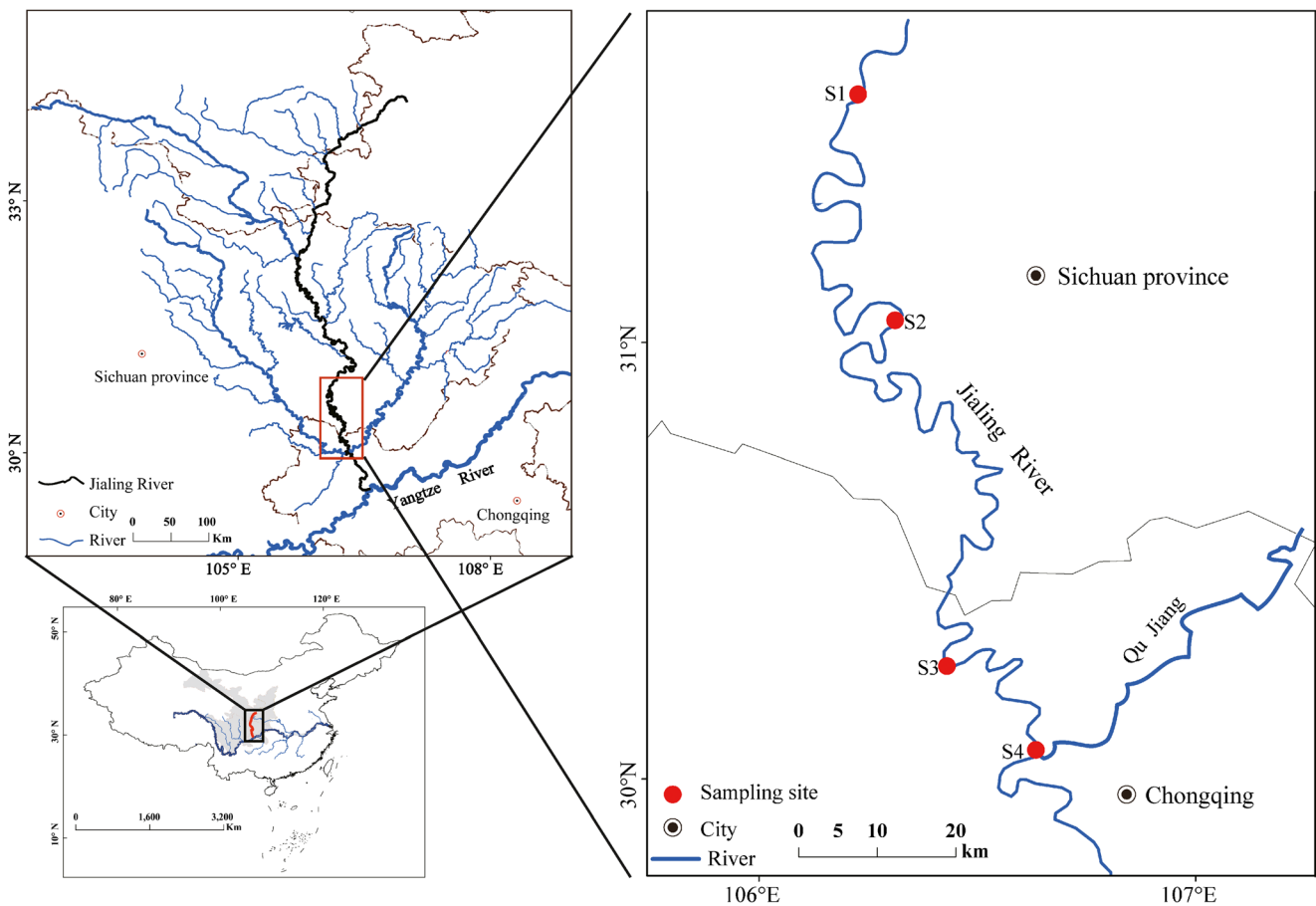
**Fig. 1** Location of four sampling sites in Jialing River

$$M = \frac{C_e(V_{gel} + V_{acid})}{f_e} \tag{1}$$

where $C_e$ is the concentration of the metal in the eluted solution; $V_{gel}$ and $V_{acid}$ are the volumes of the binding gel and the extracted acid added for elution, respectively; and $f_e$ is the elution factor (0.8) (Zhang and Davison 1995).

The average concentration of $C_{DGT}$ (μg L$^{-1}$) was calculated based on the mass ($M$, μg) accumulated on the gel and the thickness of the diffusive path length, according to Eq. (2):

$$C_{DGT} = \frac{M \Delta g}{DtA} \tag{2}$$

where $\Delta g$ is the thickness of the diffusive gel and membrane filter (cm); $D$ is the diffusion coefficient of the target analyte in the diffusive gel and prefilter (cm$^2$ s$^{-1}$); $t$ is the duration of the deployment (s); and $A$ is the area of the sampling window (cm$^2$).

## Flux calculation

To evaluate the transfer of Cu and Zn across the geochemical interfaces, the apparent fluxes of Cu and Zn across the sediment-water interface (SWI) were calculated using a numerical model

developed by Guan et al. (2016); this model is based on the sediment properties, and the equation is as follows:

$$F = F_w + F_s = Dw\left(\frac{\partial CDGT}{\partial Xw}\right)(x = 0) + \phi Ds\left(\frac{\partial CDGT}{\partial Xs}\right)(x = 0) \tag{3}$$

where $F$ is the total flux of Cu and Zn across the interface, $F_w$ is the labile Cu and Zn flux from the water to the SWI, $F_s$ represents the labile Cu and Zn fluxes from the sediment to the SWI, Φ is the porosity of the sediment with a value of 0.9 based on the study by Ding et al. (2015), $D_w$ is the matrix-specific diffusion coefficient of Cu and Zn in the overlying water, $D_s$ ($\varphi^2 \times D_w$) is the matrix-specific diffusion coefficient of Cu and Zn in the sediment (Ullman and Aller 1982), $\left(\frac{\partial CDGT}{\partial Xw}\right)$ $(x = 0)$ is the DGT concentration gradient in the overlying water, and $\left(\frac{\partial CDGT}{\partial Xs}\right)$ $(x = 0)$ is the DGT concentration gradient in the sediment.

## Sediment quality guidelines and risk assessment code

Sediment quality guidelines (SQGs) have been proven to be a quick, powerful tool for assessing the risk of heavy metal contamination in sediments (MacDonald et al. 2000). In this

**Table 1** Exchangeable fraction of Cu and Zn in four sites and risk assessment code (RAC) (Perin et al. 1985)

| Metal | S1 | S2 | S3 | S4 |
|---|---|---|---|---|
| Cu | 2.5 | 7.9 | 1.9 | 1.6 |
| Zn | 3.0 | 1.8 | 2.7 | 2.1 |
| Risk | Metal in the exchangeable fraction (%) | | | |
| No | < 1 | | | |
| Low | 1–10 | | | |
| Medium | 11–30 | | | |
| High | 31–50 | | | |
| Very | > 50 | | | |

study, four types of limit values were applied to assess the potential environmental risk to the ecosystem based on the total concentration of Ni, including the Chinese sediment quality guideline Class I (CSQG I), the Chinese sediment quality guideline Class II (CSQG II), the threshold effect concentration (TEC), and the probable effect concentration (PEC) (Long and MacDonald 1998; CEPA 2002; Feng et al. 2011). In addition, the risk assessment code (RAC) was applied to evaluate the risk and mobility of the exchangeable and carbonate fractions of Cu and Zn in the sediments (Perin et al. 1985; Singh et al. 2005; Ke et al. 2017). These fractions are considered to be weakly bonded metals that may equilibrate with the aqueous phase and thus rapidly become more bioavailable than they were in the solid phase (Pardo et al. 1990). The RAC classification for assessing Cu and Zn pollution is presented as the percentage of the acid-soluble fraction in the sediment (Table 1).

## BCR sequential extraction and acid digestion

The application of a modified three-step BCR method, and acid digestion was used to differentiate the Cu and Zn fractions in the surface sediment (Pueyo et al. 2008). A 0.50-g sample of dried surface sediment was weighed and added to a series of solutions to extract the four fractions of heavy metals: the acid-soluble/exchangeable fraction (F1), reducible fraction (F2), oxidation fraction (F3), and residual fraction (F4). The details of the extraction scheme are listed in Table 2. The filtrate of all the fractions was analyzed via ICP-MS (Thermo Fisher Scientific, X SERIES, USA). Total metal concentrations in sediments were digested following Ščančar et al. (2000): $0.300 \pm 0.001$ g dry sediment samples were first soaked in 2 mL of $HNO_3$ for 24 h overnight at room temperature and then digested with 12 mL of a mixture of perchloric and nitric acid (1:3) in a sand bath until the solution became faint yellow. The solution was then concentrated to approximately 1–2 mL and spiked with 10 mL of hydrofluoric acid; the solution was again evaporated and concentrated to 1–

2 mL. The filtrate of all the fractions and total fraction were then diluted and analyzed via ICP-MS (Thermo Fisher Scientific, X SERIEPS, USA).

## Data analysis

Statistical analysis was conducted using Microsoft Excel 2016 and SPSS 23.0. Pearson's correlation analysis was employed to assess the correlations among Cu, Zn, and Fe. The figures were plotted with OriginPro 9. The map of the study area was plotted with ArcGIS 10.0.

## Results and discussion

### Fractions of Cu and Zn in the sediments

The results of the BCR sequential extraction are presented in Fig. 2. The fractions of Cu and Zn showed similar trends at the four sites. A large quantity of Cu and Zn was bound in F2 (Cu, 9.9–49.3%, mean: 33.0%; Zn, 9.2–45.5%, mean: 31.6%) and F4 (Cu, 47.8–85.7%, mean: 62.21%; Zn, 48.5–72.6, mean: 54.7%), which represented over 90% on average of the total concentrations in the sediment at the four sites. Conversely, less than 4% (means of 3.5% for Cu and 2.4% for Zn) was bound in F1, and 1.1% and 11.2% were bound in F3 on average for Cu and Zn, respectively. F1 is thought to be the bioavailable fraction that can be readily taken up by aquatic organisms. In addition, F2 is thought to have a high potential for transformation into the F1 fraction if the sediment environment changes (e.g., in response to variations in Eh or pH) (Shen et al. 2017; Xu et al. 2016). The above results show that the percentages of F1-Cu and F1-Zn were low, whereas F2-Cu and F2-Zn represented over 30% of the total. Thus, it could be inferred that although the bioavailability of Cu and Zn was not high, there was a potential risk of these metals becoming bioavailable. This result is consistent with the findings of a previous study, which reported that in the upstream section of the Jialing River near a Pb-Zn smelter (Shen et al. 2017), Cu and Zn are present in the highly exchangeable and mobile fractions. Furthermore, a similar distribution of Cu and Zn was observed in the various fractions. Cu and Zn are both divalent ions and have similar chemical characteristics. For example, when $Cu^{2+}$ and $Zn^{2+}$ in wastewater are discharged into the Jialing River and finally settle in the sediments, they may both be captured by iron/manganese oxides, organic matter, or sulfur (once strong reducing conditions form) to form stable chemical substances. Hence, it can be inferred that the similar distributions of Cu and Zn in different fractions are related to the chemical characteristics of the two metals and their origin from the same trace source.

**Table 2** Reagents used and extraction procedures of sediments

| Procedure | Reagents | Method | Fraction |
|---|---|---|---|
| 1 | 0.11 M CH$_3$COOH | Samples were shaken for 16 h at $20 \pm 2$ °C and then centrifuged at 3500$g$ for 20 min | Exchangeable and acid soluble fraction |
| 2 | 0.5 M NH$_2$OH·HCl (pH = 2.0) | Samples were shaken for 16 h at $20 \pm 2$ °C and then centrifuged at 3500$g$ for 20 min | Reducible fraction |
| 3 | (1) 8.8 M H$_2$O$_2$ (2) NH$_4$OAC (pH = 2.0–3.0) | (1) Samples were firstly soaked with 8.8 M H$_2$O$_2$ at room temperature for 1 h with occasional shaking, following by a 1 h digestion at $85 \pm 2$ °C. The solution was concentrated to at least 3 mL and respiked with 8.8 M H$_2$O$_2$ for a further digestion until the solution reached approximate 1 mL. (2) the above samples were then spiked with 1 M NH$_4$OAC and shaken for 16 h at $20 \pm 2$ °C and then centrifuged at 3500 g for 10 min. | Oxidizable fraction |
| 4 | 37%HCl + 70%HNO$_3$ | Samples were digested with 37%HCl and 70%HNO$_3$ with a volume ratio 3:1 for 2 h at $160 \pm 2$ °C in a graphite oven | Residual fraction |

## Environmental risk assessment using SQGs and RAC

In this study, two approaches, the SQGs and RAC, were used to assess the environmental risk of Cu and Zn in the sediment of the study area. Four empirical SQGs and the total concentrations of Cu and Zn are displayed in Table 3, and a comparison of the total Cu and Zn with the SQGs is shown in Fig. 3. The total concentrations of Cu and Zn ranged from 56.30 to 93.10 mg kg$^{-1}$ and 167.40 to 278.81 mg kg$^{-1}$, respectively. The total concentrations of Cu (C$_{total}$-Cu) and Zn (C$_{total}$-Zn) followed the same order at the four sites: S3 > S2 >S4 > S1. The SQG evaluation was based on the total concentration of heavy metals. According to the evaluation standards of CEPA (2002) and MacDonald et al. (2000), CSQG I and TEC (low range values) represent the concentrations below which adverse effects on the aquatic ecosystem are not expected; the water in this area is suitable for propagation industries and natural reserves. CSQG II and PEC represent the concentrations above which adverse effects are expected to occur, and the water quality is suitable only for transport. Concentrations between these values indicate that adverse effects may occur occasionally, and the water in this area is suitable for tourism. The C$_{total}$-Cu and C$_{total}$-Zn at all four sites were significantly higher than the CSQG I and TEC limits but not above the CSQG II and PEC limits, indicating that Cu and Zn may pose a toxicity risk to aquatic systems in the downstream section of the Jialing River. The exchangeable fractions are considered to contain weakly bound metals that may equilibrate with the aqueous phase, thus rapidly becoming more bioavailable than they were in the solid phase (Pardo et al. 1990). The SWI is a unique area, and different heavy metal fractions may make different contributions to the level of toxicity affecting the ecosystem (Tang et al. 2014). Hence, the RAC, which is based on the bioavailable fraction, could provide a more accurate representation than the SQGs of Cu and Zn pollution in the study area. The RAC divides environmental risk into five ranges: no risk, low risk, medium risk, high risk, and very high risk. The percentages of F1-Cu and F1-Zn based on the results of BCR sequential extraction are exhibited in Table 1. Based on the five levels of the RAC (Perin et al. 1985),
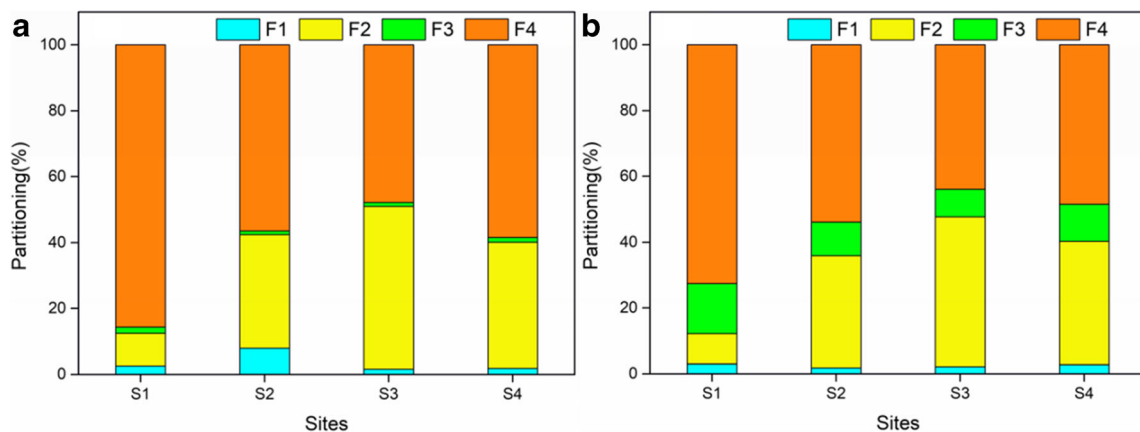


**Fig. 2** The fraction of Cu (**a**) and Zn (**b**) in the sediment (blue ■, yellow □, green ■, and orange □ rectangles represent fraction F1, F2, F3, and F4 respectively)

**Table 3** Total metal concentrations in four sites and four empirical SQGs (mg kg$^{-1}$)

|    | S1 | S2 | S3 | S4 | CSQG I | CSQG II | TEC | PEC |
|----|------|--------|--------|--------|--------|---------|------|-----|
| Cu | 56.30 | 81.58 | 93.10 | 61.15 | 35 | 100 | 31.6 | 149 |
| Zn | 167.40 | 257.25 | 278.81 | 238.57 | 150 | 350 | 121 | 459 |

CSQGs I, Chinese Sediment Quality Guidelines, Class I; CQGs II, Chinese Sediment Quality Guidelines, Class II. CEPA 2002

TEC, threshold effect concentration; PEC, probable effect concentration. MacDonald et al. 2000

because both F1-Cu and F1-Zn were below 10%, Cu and Zn presented a low environmental risk. In summary, the results of both the SQGs and RAC demonstrated that the environmental risk of Cu and Zn in the downstream section of the Jialing River was low.

## Vertical variations in $C_{DGT}$-Cu, $C_{DGT}$-Zn, and $C_{DGT}$-Fe

The vertical distributions of Cu, Zn, and Fe at the four sites are presented in Fig. 4. At S1, $C_{DGT}$-Cu decreased from 8.82 μg kg$^{-1}$ at 3 cm in the overlying water to 0 μg kg$^{-1}$ at 0.5 cm and at the SWI. The level then increased steadily until − 11 cm, where the concentration increased sharply from 12.59 μg kg$^{-1}$ to 36.29 μg kg$^{-1}$ between − 11 cm and − 12 cm. A similar trend was observed for Zn from 3 cm in the overlying water (82.06 μg kg$^{-1}$) to the SWI (42.33 μg kg$^{-1}$); $C_{DGT}$-Zn then fluctuated until − 10.5 cm, where a sharp increase was observed between − 10.5 cm (38.62 μg kg$^{-1}$) and − 12 cm (125.43 μg kg$^{-1}$). $C_{DGT}$-Fe maintained an average value of 1000.00 μg L$^{-1}$ from 3 cm to the SWI and then showed a slight increase from the SWI (1072.30 μg L$^{-1}$) to − 1.5 cm (1362.61 μg L$^{-1}$). A peak was observed at − 3 cm (2084.94 μg L$^{-1}$), and then there was a steady decrease to the bottom of the DGT probe. At S2, $C_{DGT}$-Cu showed a slow decrease from 3 cm to the SWI and then a steady increase from the SWI to − 8 cm. Below − 8 cm, there was a small peak (44.52 μg kg$^{-1}$) at − 8.5 cm and a noticeable peak (71.06 μg kg$^{-1}$) at − 11 cm. For Zn, a clear valley

(8.76 μg kg$^{-1}$) was observed at the SWI. The curve then maintained a continual, steady increase to the bottom of the probe. A clear peak in the $C_{DGT}$-Fe curve was observed at the SWI (2950.12 μg L$^{-1}$), and the level fluctuated until − 7.5 cm. Another broad peak was observed at − 9.5 cm (2645.18 μg L$^{-1}$), and then there was a decrease from − 9.5 cm to the bottom of the probe. At S3, $C_{DGT}$-Cu showed an increase from 17.70 μg kg$^{-1}$ (3 cm) in the overlying water to 43.56 μg kg$^{-1}$ (0.5 cm) and then fluctuated until − 8.5 cm, where there was a rapid increase from − 8.5 cm (15.76 μg kg$^{-1}$) to the bottom of the DGT probe (125.85 μg kg$^{-1}$). Similar to Cu, $C_{DGT}$-Zn fluctuated from 3 to − 9.5 cm, followed by a sharp increase from 103.14 μg kg$^{-1}$ to 535.01 μg kg$^{-1}$. The M-shaped $C_{DGT}$-Fe curve showed twin peaks at 1.5 cm (2637.74 μg L$^{-1}$) and − 1 cm (2510.81 μg L$^{-1}$). The level then fluctuated until a third broad peak appeared at − 9 cm (2627.15 μg L$^{-1}$). A sharp decrease was then observed from − 9.5 to − 10 cm. At S4, $C_{DGT}$-Cu decreased from 9.21 μg L$^{-1}$ in the overlying water to 2.19 μg L$^{-1}$ at SWI. The curve then fluctuated until a prominent peak was obtained at − 10 cm (16.5 μg L$^{-1}$). $C_{DGT}$-Zn initially fluctuated in the overlying water and then decreased across the SWI. In the sediments, the curve showed a rising wave shape and two low peaks were obtained at − 3.5 cm (36.21 μg L$^{-1}$) and − 9 cm (49.59 μg L$^{-1}$). $C_{DGT}$-Fe maintained a low concentration in the overlying water followed by a rapid increase to 655.1 μg L$^{-1}$ at the SWI. The level then fluctuated from − 0.5 to − 6.5 cm to three peaks at − 7 cm (828.2 μg L$^{-1}$), − 8.5 cm (841.8 μg L$^{-1}$), and − 11.5 cm (880.5 μg L$^{-1}$), followed by a sharp decrease to 0.08 μg L$^{-1}$ at the bottom of the DGT probe.

The above results showed that the vertical distributions of Cu and Zn were quite similar. The most obvious trend was that both exhibited a significant increase at the bottom of the sediment cores. Further analysis of $C_{DGT}$-Cu and $C_{DGT}$-Zn found that these two metals were significantly positively correlated (Fig. 5, $r = 0.834$, $p < 0.01$). Combined with the similar distributions of $C_{total}$-Cu and $C_{total}$-Zn at the four sites discussed above, these two results indicate that Cu and Zn had similar horizontal and vertical distributions. Thus, the
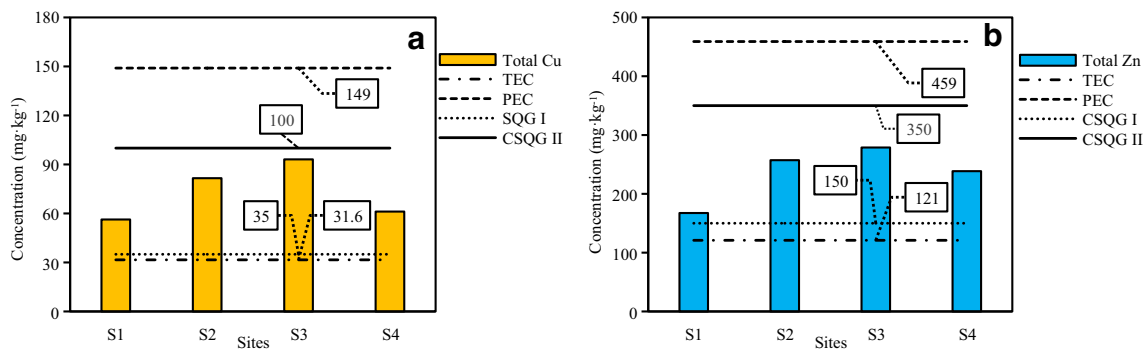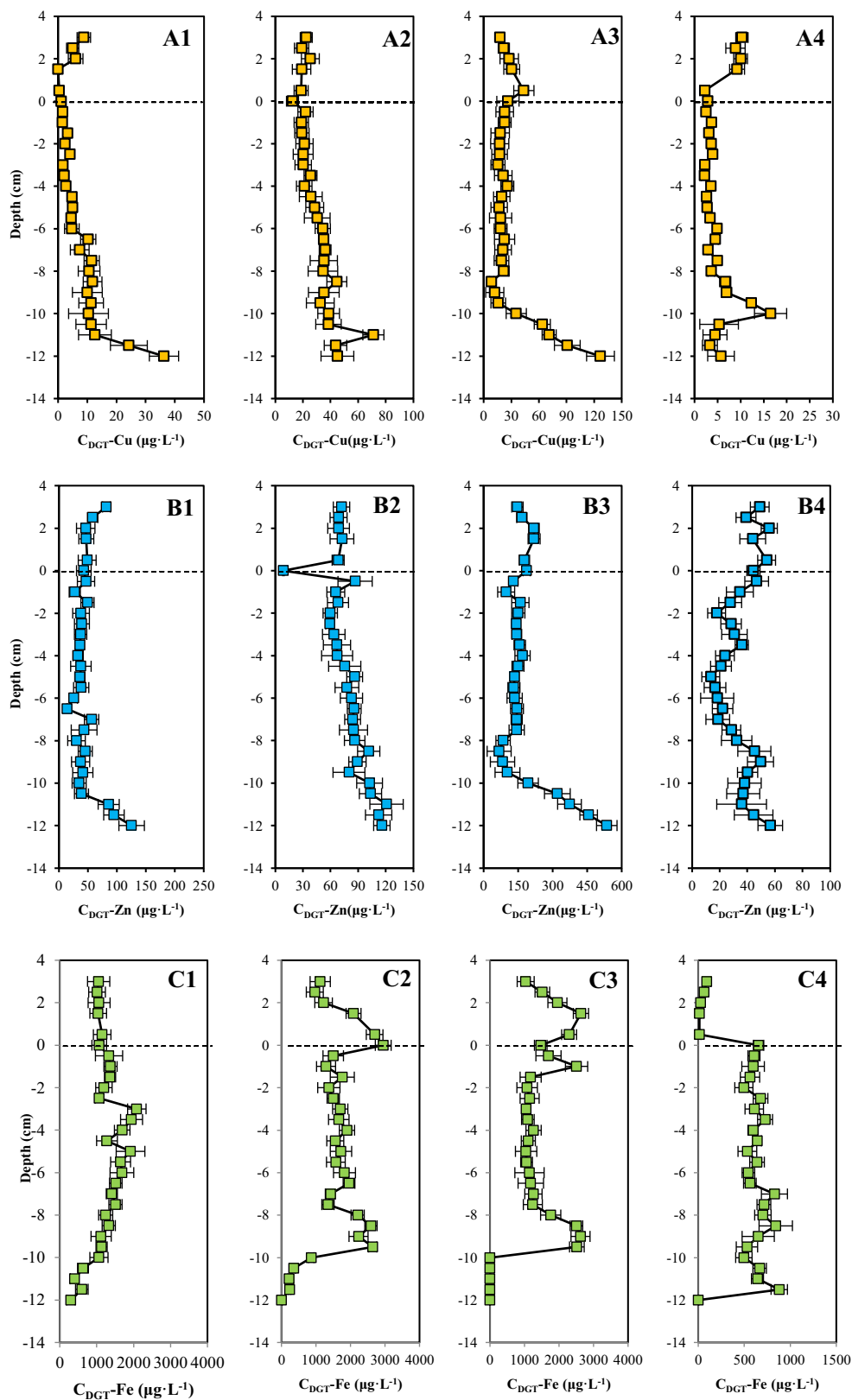


**Fig. 3** Comparison of total concentration of Cu (**a**) and Zn (**b**) with four empirical SQG values

**Fig. 4** Vertical distribution of DGT-Cu (A1–A4 represent S1 to S4, the same below), DGT-Zn (B1–B4), and DGT-Fe (C1–C4) in the four sites sediment cores



two metals probably had the same source and this source may be related to the anthropogenic input of large amounts of metals from Pb-Zn mining and smelting. A case study

claimed that the mining of Zn and Pb may also cause Cd and Cu contamination in the soil and sediment in the upstream section of the Jialing River. Wang et al. (2017a) also

found that Cu and Zn were significantly correlated ($r = 0.671$, $p < 0.01$) in the soils of a mining area in Sichuan Province. Therefore, the simultaneous input of Cu and Zn to the sediment of the Jialing River may originate from Zn-Pb mining in the upstream section.

A comparison of the vertical distributions of Zn and Cu with Fe indicates (Fig. 4) that the variation in $C_{DGT}$-Fe exhibited an inverse trend relative to that of $C_{DGT}$-Cu and $C_{DGT}$-Zn. This finding indicates that the release of Cu and Zn may be related to Fe. The sequential extraction results also revealed that large amounts of Cu and Zn were bound in the F2 fraction (the iron oxide fraction). Previous studies have also found that the release of labile Fe was inversely correlated with the release of heavy metals, including cadmium (Cd), antimony (Sb), vanadium (V), and arsenic (As) (Xu et al. 2016; Gao et al. 2016, 2017a, 2017b; Yan et al. 2018). Thus, further study is needed, e.g., a correlation analysis between $C_{DGT}$-Fe and $C_{DGT}$-Cu/Zn.

## Apparent flux of Cu and Zn at the SWI

The calculation of trace metal diffusive fluxes at the SWI is important for determining the mobilization trend across the SWI and for determining whether the sediment is a source or sink for contaminants (Tang et al. 2016; Gao et al. 2017a). Data at the millimeter scale of the DGT probe can provide more precise values than those at a larger scale to evaluate the apparent flux of Cu and Zn at the SWI. Figure 6 shows the apparent fluxes of Cu ($F_{Cu}$) and Zn ($F_{Zn}$) across the SWI at the four sites. The negative and positive values represent fluxes to the sediment and water, respectively (Ding et al. 2015; Xu et al. 2016). In this study, $F_{Cu}$ and $F_{Zn}$ ranged from $-1.85$ to $62.35$ ng cm$^2$ day$^{-1}$ and $11.76$–$190.47$ ng cm$^2$ day$^{-1}$, respectively. At S2, S3, and S4, $F_{Cu}$ had positive values, indicating that the Cu at these three sites was mobilized from the sediments to the water, and the sediment could be identified as a source with the potential risk of Cu release to the overlying water. The flux value at S1 had a

negative value, indicating that Cu could flux from the overlying water into the sediment and that the sediment may be a sink for Cu. For Zn, the $F_{Zn}$ values at all the sites had positive fluxes, which indicates that all four sites in the study area are a source of Zn release. Furthermore, the $F_{Cu}$ and $F_{Zn}$ values at S3 were significantly higher than those at the other sites ($p < 0.05$), indicating that the speed of Cu and Zn mobilization from the sediment to the overlying water was the most rapid at S3. This result correlated well with the DGT result ($C_{DGT}$-Cu and $C_{DGT}$-Zn in the sediment at S3 were much higher than those at the other three sites). The flux results further suggested that sediments at S3 had a high potential to release Cu and Zn to the aquatic ecosystem and that among the studied sites, the aquatic ecosystem at S3 was the most vulnerable to Cu and Zn contamination.

## Key factors affecting the remobilization of Cu and Zn in sediments

### The effect of Fe release on the remobilization of Cu and Zn

The above results clearly demonstrated that Cu and Zn had very similar trace sources and were possibly transported from upstream areas. What are the factors that caused the release of labile Cu and Zn? Iron oxides have been widely accepted as substantial sinks for heavy metals, such as Cu, Zn, Cd, and Pb. Iron oxides may adsorb metals via bidentate bonding [reaction (1)] or simultaneous adsorption and hydrolysis at pH 7.0 [reaction (2)] (Benjamin and Leckie 1981):

$$2FeOH + Me^{2+} = Fe_2O_2Me + 2H^+ \quad (1)$$

$$FeOH + Me^{2+} + H_2O = FeOMeOH + 2H^+ \quad (2)$$
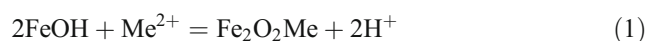
As the total concentration of Mn in this study was only 5% of the Fe concentration, the overall contribution of Mn oxides to adsorption was negligible due to their low abundance in the sediments. Thus, we first hypothesized that Fe may have been a key factor that mitigated this process. Significant negative correlations were obtained at S1 ($r_{Cu} = -0.610$, $p < 0.01$; $r_{Zn} = -0.684$, $p < 0.01$), S2 ($r_{Cu} = -0.474$, $p < 0.05$; $r_{Zn} = -0.583$, $p < 0.01$), S3 ($r_{Cu} = -0.594$, $p < 0.01$; $r_{Zn} = -0.664$, $p < 0.01$), and S4 ($r_{Cu} = -0.412$, $p < 0.05$; $r_{Zn} = -0.483$, $p < 0.01$) (Fig. 7). Fe release from the sediment was primarily due to the reductive dissolution of iron oxides (such as ferrihydrite, goethite, or hematite) under highly reducing conditions, and Fe(II) may have been the main driving force of this process (Vodyanitskii 2010; Nielsen et al. 2014; Zhang et al. 2018, 2019). Once the reduced condition is altered, for example, if oxygen is introduced into deep sediment, the reductive dissolution of Fe oxides may be hindered. Zhang et al. (2018) and Zhang et al. (2019) found that in soils with iron oxide in a relatively poorly crystalline phase, more DGT-labile Fe could be captured by the DGT sampler under partially reducing
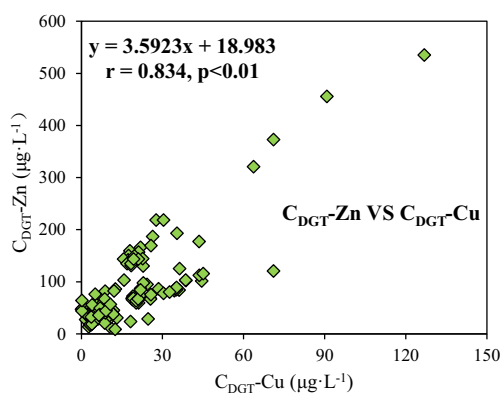


Fig. 5 The relationship between $C_{DGT}$–Zn and $C_{DGT}$–Cu measured in four sediment cores at varied depths

y = 3.5923x + 18.983
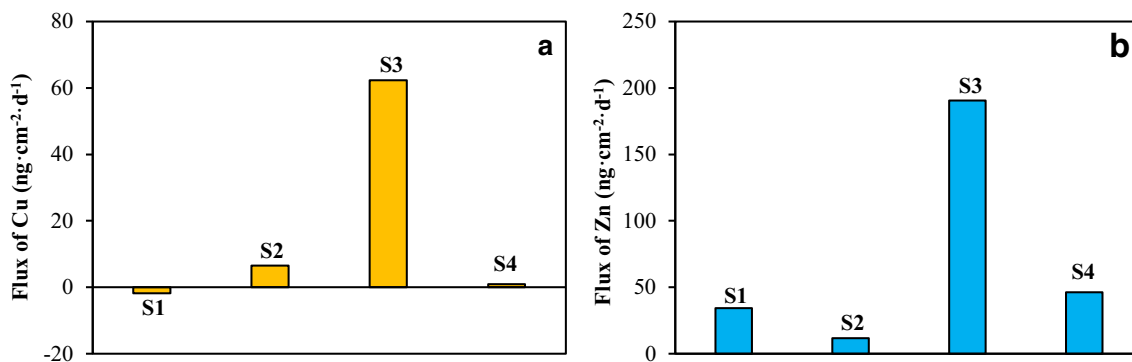r = 0.834, p<0.01

$C_{DGT}$-Zn VS $C_{DGT}$-Cu

**Fig. 6** Apparent diffusion fluxes of Cu (**a**) and Zn (**b**) across the SWI (the negative and positive values represent fluxes to the sediment and water, respectively)

conditions. Casagrande et al. (2005) also pointed out that there was an increase in the Zn adsorbed by soil rich in Fe oxides. Thus, we hypothesized that under the highly reducing conditions of the sediments, more DGT-labile Fe would be released, more iron oxides would exist at the corresponding depth, and more heavy metals would be trapped by the iron oxides. A non-simultaneous release of Fe and metals occurred primarily because the surface area of the iron oxides was still sufficient to adsorb Zn and Cu. The average ratios of $C_{DGT}$-Zn/$C_{DGT}$-Fe and $C_{DGT}$-Cu/$C_{DGT}$-Fe were less than 0.02 and 0.05, respectively, indicating that the iron oxides still had sufficient adsorption sites to capture the heavy metals. Hence, the remobilization of Cu and Zn controlled by Fe tended to reflect a chemical or physical desorption process. From the above discussion, we hypothesized that $C_{DGT}$-Fe may have been a key factor controlling the release of Cu and Zn from the sediments in the study area.

### The effect of S release on the remobilization of Cu and Zn

The BCR results showed that approximately 3% of Cu and 11% of Zn were bound to the organic matter/sulfide fraction (F3 fraction). It is widely accepted that sulfur (S) also plays an important role in controlling the reactivity, toxicity, and mobility of heavy metals in sediments (Tsai et al. 2003; Seidel et al. 2006; Yin et al. 2008). As the average total organic carbon (TOC) content at the four sites was only 1.4%, we hypothesized that the rapid increase at the bottom (approximately − 9 cm to − 12 cm) of the probe was not regulated by Fe alone; the DGT results provide evidence that S may be another factor that can significantly mitigate the release of Cu and Zn. This study applied an AgI gel to the DGT probe to measure dissolved sulfides, such as HS− and H2S (Wu et al. 2015; Xu et al. 2016), to study the mechanism by which S affects the release of Cu and Zn. During DGT probe deployment, sulfide species from interstitial water react with the pale yellow AgI to form black As2S (Stockdale et al. 2009; Xu et al. 2016). The intensity of the darkness of the AgI gel can be photographed for analysis. In this study, we selected S3

(with the highest $C_{DGT}$-Cu and $C_{DGT}$-Zn) to study the change in sulfides along the DGT probe. A hotspot of $C_{DGT}$-Cu and $C_{DGT}$-Zn was clearly observed at the bottom of the probe from approximately − 10 cm to − 12 cm, and the AgI gel also exhibited a prominent dark area at the same depth (Fig. 8). These results indicate that the simultaneous release of Cu-Zn and S occurred at this depth. This result is consistent with the results of previous studies (Gao et al. 2015; Xu et al. 2016; Gao et al. 2017a) on other heavy metals. Gao et al. (2015) found a simultaneous release of S and heavy metals below − 11 cm.

Under highly reducing conditions, cations normally bind with $S^{2-}$ and form highly insoluble sulfide precipitates in the sediment (Yin et al. 2008). Cu and Zn can generally substitute for Fe in FeS to form highly insoluble metal sulfide precipitates (under conditions with an Eh lower than − 150 mV and a pH ranging from 7–7.5) via reactions (3) and (4) (Di Toro et al. 1992; Tankere-Muller et al. 2007; Badrzadeh et al. 2011., Zhang et al. 2013; Zhu et al. 2018):

$$Cu^{2+} + FeS = CuS(s) + Fe^{2+} \qquad (3)$$

$$Zn^{2+} + FeS = ZnS(s) + Fe^{2+} \qquad (4)$$
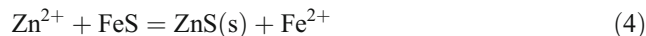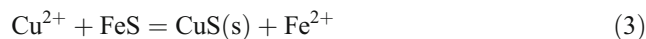
Dissolved Cu and Zn thus normally remained at low concentrations in the sediments because with an excess of acid volatile sulfur (AVS), sediments typically have very low concentrations of dissolved metals in their pore water (Di Toro et al. 1992; Simpson et al. 2000). Nevertheless, insoluble sulfide precipitates may become much more vulnerable if the aquatic environment changes and S and metals are released from the sediment. The simultaneous release of S with Cu-Zn may be related to the instability of sulfides. The stabilities of CuS and ZnS are normally altered by changes in the sediment redox state. Investigations have concluded that heavy metals bound to S can be liberated during the aeration of sediments. This is primarily caused by the introduction of oxygen and the substantial increase in the bioavailability of Cu and Zn in sediments (Schaanning et al. 1996). A possible interpretation is that Cu and Zn may experience a dissolution process similar to cadmium (Cd) (Wang et al. 2010) by both biotic and abiotic

**Fig. 7** Correlation analysis between $C_{DGT}$–Fe and $C_{DGT}$–Cu (A1–A4 represent S1 to S4, the same below), $C_{DGT}$–Fe and $C_{DGT}$–Zn (B1–B4)
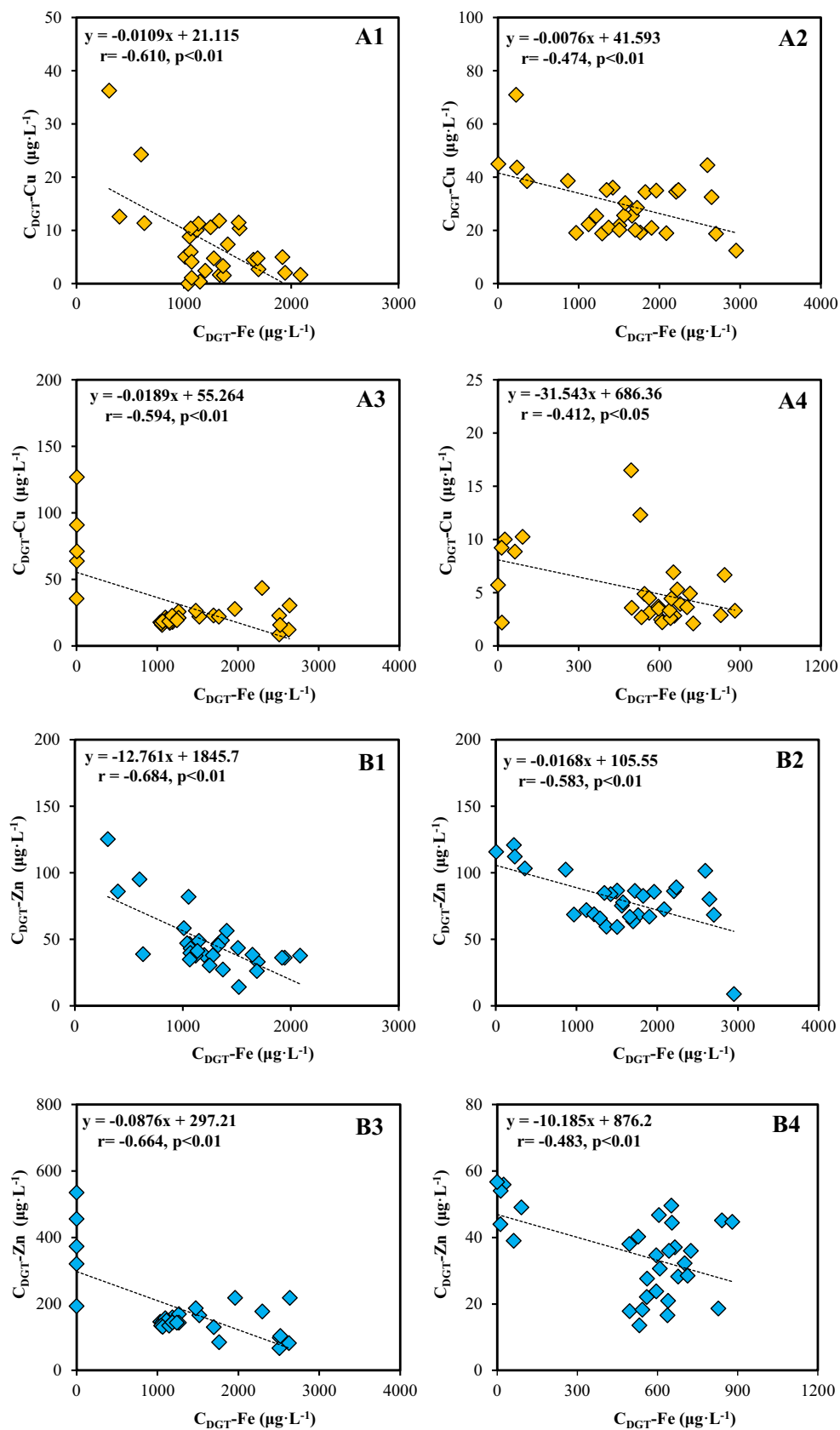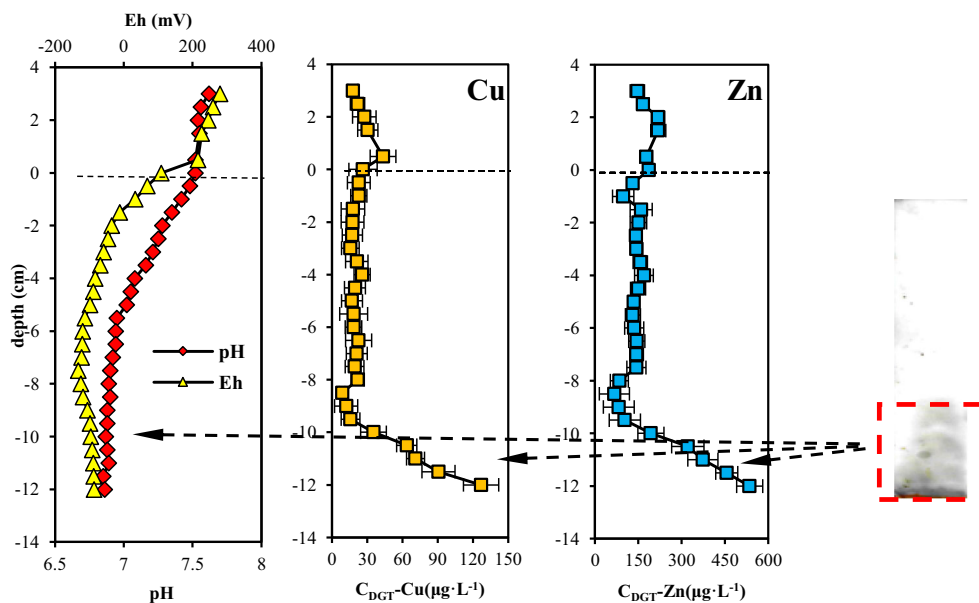
**Fig. 8** Vertical profiles of pH and Eh in sediment core, greyscale image of AgI gel and the corresponding "hotspot" of Chelex gel at S3 (yellow triangle and red diamond represent Eh and pH respectively)

processes in the study area; $C_{DGT}$-Cu and $C_{DGT}$-Zn in precipitates at the bottom were partially oxidized to soluble $CuSO_4$ and $ZnSO_4$ via the following reactions:

$$CuS(s) + 2O_2\ (g) = Cu^{2+} + SO_4^{2-} \tag{5}$$

$$ZnS(s) + 2O_2\ (g) = Zn^{2+} + SO_4^{2-} \tag{6}$$

In this process, oxygen acts as an electron acceptor (Motelica-Heino et al. 2003), microbial activity may promote sulfur oxidization and sulfide precipitates may become unstable (Seidel et al. 2006). Hence, the remobilization of Cu and Zn controlled by S tended to indicate an oxidizing reaction,

which was different from the process controlling Fe. The variations in pH and Eh values also provided supplementary evidence explaining why this process occurred at the bottom of the probe (especially at − 8 to − 12 cm) (Fig. 8). Although the Eh values decreased rapidly below the SWI, they increased from − 6.5 to − 12 cm. We hypothesized that this unusual phenomenon may be related to the possible introduction of $O_2$. De Jonge et al. (2012) thought that an increase in $O_2$ may change the Eh, leading to the oxidation of S and the release of some S-bound stable-phase metals to the pore water. The pH also exhibited a steady decreasing trend from 6 to − 12 cm. This observation also suggested that the introduction
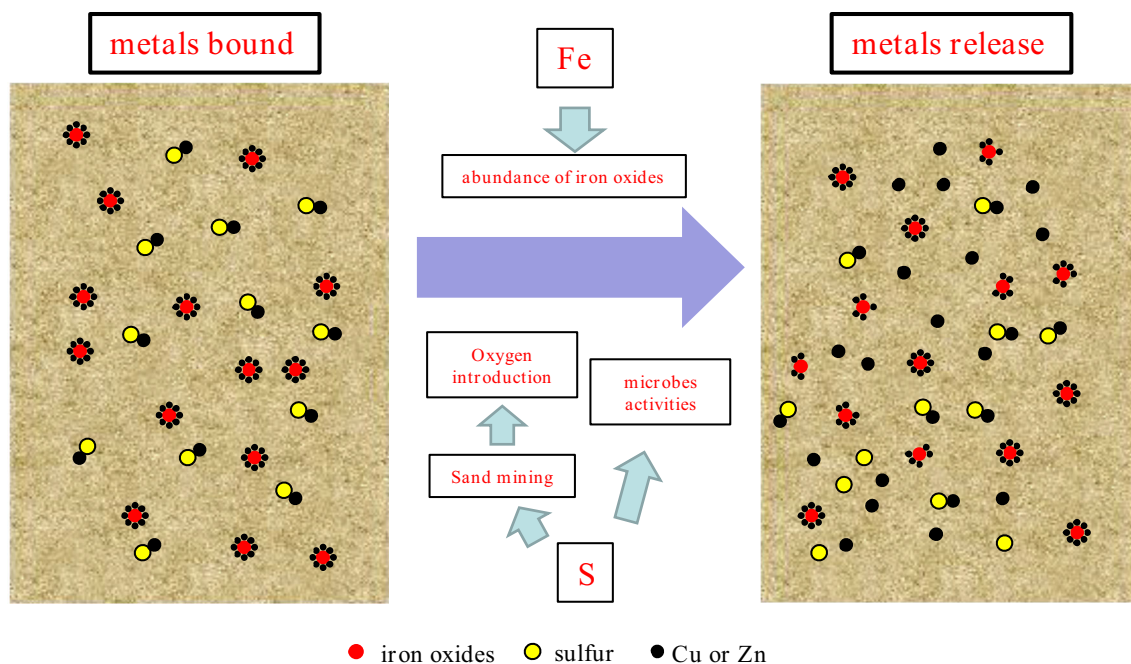
**Fig. 9** Conceptual model of Cu and Zn release in the sediments

of $O_2$ may have hindered the Fe oxide reductive dissolution process in the deep sediment and that the decrease in Fe(II) concentration could further diminish the water ionization process (Wang et al. 2017b; Zhang et al. 2018). Accordingly, fewer protons may have caused a slower and stable decreasing pH trend at the bottom of the sediment in contrast to the fast decrease in the surface sediment. The above Eh and pH results may also explain the phenomenon and our hypothesis why $C_{DGT}$-Fe presented a much lower concentration, while $C_{DGT}$-Cu/Zn showed a higher concentration in the deep sediment, which may have been related to the introduction of $O_2$ (Fig. 7).

Actually, the S3 sampling site has a history of sand mining for 0.5–1 year. The intensive sand mining activity in the downstream section of the Jialing River may strongly and directly influence the stability of sulfides. Sand mining may cause a substantial introduction of oxygen into deeper sediments and alter the redox conditions of the sediment. No sharp increase in Eh was observed in the S3 sediment core, probably because the sediments had equilibrated for a long period. However, the abnormal gradual increases in Eh and pH in the deep sediment still indicated that sand mining had impacted the sediments at this site. The topography in the downstream region of the study area (S3 and S4) is relatively flat, whereas S1 and S2 are associated with mountainous topography. A high water velocity may cause the influx of large amounts of sediment from upstream areas, which may gradually cover the excavated holes and store trace oxygen in the micropores in the sediments. The tiny amounts of oxygen in micropores may lead to a gradual increase in sediment Eh and continual Cu and Zn release from the sediments. This anthropogenic activity may override the effect of resident microbial activity and cause the release of S and heavy metals. A conceptual model was developed to describe how Fe and S can mitigate Cu and Zn release processes in sediment (Fig. 9).

## Conclusions

In this study, we evaluated the environmental risk and studied the fractions and remobilization of Cu and Zn in sediments. Cu and Zn in the downstream section of the Jialing River presented a low environmental risk, indicating that they may not pose a serious threat to the aquatic ecosystem. Cu and Zn were primarily bound in the F2 and F4 fractions. Both the horizontal (total concentrations at four sites) and vertical distribution (DGT) results revealed that Cu and Zn had a significant positive correlation, indicating that they may have the same anthropogenic source from upstream. The DGT results also showed significant remobilization of Cu and Zn from the sediments, which is thought to be related to Fe (fraction 2) and S (fraction 3). A further correlation analysis found that $C_{DGT}$-Cu/Zn had a negative correlation with $C_{DGT}$-Fe, and thus, Cu

and Zn release may be mitigated by the abundance of iron oxides in the sediment. In addition, the "dark area" of the AgI gel correlated with the "hotspot" of the Chelex gel that measured Cu and Zn, indicating that S may be released simultaneously. In summary, the DGT technique was proven to be a robust tool for monitoring and studying the mechanism of Cu and Zn release from sediment. Although Cu and Zn were assessed as presenting a low environmental risk to the aquatic ecosystem, the sand mining industry is suggested to significantly influence sediment redox and accelerate the release of Cu and Zn from sediments, which needs to be considered by the government.

## References

Akcay H, Oguz A, Karapire C (2003) Study of heavy metal pollution and speciation in Buyak Menderes and Gediz river sediments. Water Res 37(4):813–822

Badrzadeh Z, Barrett TJ, Peter JM, Gimeno D, Sabzehei M, Aghazadeh M (2011) Geology, mineralogy, and sulfur isotope geochemistry of the Sargaz Cu–Zn volcanogenic massive sulfide deposit, Sanandaj–Sirjan Zone, Iran. Mineral Deposita 46(8):905–923

Benjamin MM, Leckie JO (1981) Multiple-site adsorption of Cd, Cu, Zn, and Pb on amorphous iron oxyhydroxide. J Colloid Interface Sci 79(1):209–221

Buzier R, Charriau A, Corona D, Lenain JF, Fondanèche P, Joussein E, Poulier G, Lissalde S, Mazzella N, Guibaud G (2014) DGT-labile As, Cd, Cu and Ni monitoring in freshwater: toward a framework for interpretation of in situ deployment. Environ Pollut 192:52–58

Casagrande JC, Alleoni LR, de Camargo OA, Arnone AD (2005) Effects of pH and ionic strength on zinc sorption by a variable charge soil. Commun Soil Sci Plan 35(15–16):2087–2095

CEPA (State Environmental Protection Administration of China) (2002) Marine sediment quality (GB 18668e2002). Standards Press of China, Beijing (in Chinese)

Dalman Ö, Demirak A, Balcı A (2006) Determination of heavy metals (Cd, Pb) and trace elements (Cu, Zn) in sediments and fish of the southeastern Aegean Sea (Turkey) by atomic absorption spectrometry. Food Chem 95(1):157–162

Dang DH, Lenoble V, Durrieu G, Omanović D, Mullot JU, Mounier S, Garnier C (2015) Seasonal variations of coastal sedimentary trace metals cycling: insight on the effect of manganese and iron (oxy) hydroxides, sulphide and organic matter. Mar Pollut Bull 92(1–2): 113–124

De Jonge M, Teuchies J, Meire P, Blust R, Bervoets L (2012) The impact of increased oxygen conditions on metal-contaminated sediments part I: effects on redox status, sediment geochemistry and metal bioavailability. Water Res 46(7):2205–2214

Di Toro DM, Mahony JD, Hansen DJ, Scott KJ, Carlson AR, Ankley GT (1992) Acid volatile sulfide predicts the acute toxicity of cadmium and nickel in sediments. Environ Sci Technol 26(1):96–101

Ding S, Han C, Wang Y, Yao L, Wang Y, Xu D, Sun Q, Williams PN, Zhang C (2015) In situ, high-resolution imaging of labile phosphorus in sediments of a large eutrophic lake. Water Res 74:100–109

Equeenuddin SM, Tripathy S, Sahoo PK, Panigrahi MK (2013) Metal behavior in sediment associated with acid mine drainage stream: role of pH. J Geochem Explor 124:230–237

Feng H, Jiang H, Gao W, Weinstein MP, Zhang Q, Zhang W, Yu L, Yuan D, Tao J (2011) Metal contamination in sediments of the western Bohai Bay and adjacent estuaries, China. J Environ Manag 92(4): 1185–1197

Fisher-Power LM, Cheng T, Rastghalam ZS (2016) Cu and Zn adsorption to a heterogeneous natural sediment: influence of leached cations and natural organic matter. Chemosphere 144:1973–1979

Gao Y, van de Velde S, Williams PN, Baeyens W, Zhang H (2015) Two-dimensional images of dissolved sulfide and metals in anoxic sediments by a novel diffusive gradients in thin film probe and optical scanning techniques. TrAC Trend Anal Chem 66:63–71

Gao L, Gao B, Zhou H, Xu D, Wang Q, Yin S (2016) Assessing the remobilization of antimony in sediments by DGT: a case study in a tributary of the Three Gorges Reservoir. Environ Pollut 214:600–607

Gao B, Gao L, Zhou Y, Xu D, Zhao X (2017a) Evaluation of the dynamic mobilization of vanadium in tributary sediments of the Three Gorges Reservoir after water impoundment. J Hydrol 551:92–99

Gao L, Gao B, Xu D, Peng W, Lu J, Gao J (2017b) Assessing remobilization characteristics of arsenic (As) in tributary sediment cores in the largest reservoir, China. Ecotoxicol Environ Saf 140:48–54

Guan DX, Williams PN, Xu HC, Li G, Luo J, Ma LQ (2016) High-resolution measurement and mapping of tungstate in waters, soils and sediments using the low-disturbance DGT sampling technique. J Hazard Mater 316:69–76

Islam MS, Ahmed MK, Habibullah-Al-Mamun M, Hoque MF (2015) Preliminary assessment of heavy metal contamination in surface sediments from a river in Bangladesh. Environ Earth Sci 73(4): 1837–1848

Ke X, Gui S, Huang H, Zhang H, Wang C, Guo W (2017) Ecological risk assessment and source identification for heavy metals in surface sediment from the Liaohe River protected area, China. Chemosphere 175:473–481

Long ER, MacDonald DD (1998) Recommended uses of empirically derived, sediment quality guidelines for marine and estuarine ecosystems. Hum Ecol Risk Assess 4(5):1019–1039

MacDonald DD, Ingersoll CG, Berger TA (2000) Development and evaluation of consensus-based sediment quality guidelines for freshwater ecosystems. Arch Environ Contam Toxicol 39(1):20–31

Motelica-Heino M, Naylor C, Zhang H, Davison W (2003) Simultaneous release of metals and sulfide in lacustrine sediment. Environ Sci Technol 37(19):4374–4381

Ndiba P, Axe L, Boonfueng T (2008) Heavy metal immobilization through phosphate and thermal treatment of dredged sediments. Environ Sci Technol 42(3):920–926

Nielsen SS, Kjeldsen P, Hansen HCB, Jakobsen R (2014) Transformation of natural ferrihydrite aged in situ in As, Cr and Cu contaminated soil studied by reduction kinetics. Appl Geochem 51:293–302

Pardo R, Barrado E, Lourdes P, Vega M (1990) Determination and speciation of heavy metals in sediments of the Pisuerga river. Water Res 24(3):373–379

Peng JF, Song YH, Yuan P, Cui XY, Qiu GL (2009) The remediation of heavy metals contaminated sediment. J Hazard Mater 161(2–3): 633–640

Perin G, Craboledda L, Lucchese M, Cirillo R, Dotta L, Zanetta ML, Oro AA (1985) Heavy metal speciation in the sediments of northern Adriatic Sea. A new approach for environmental toxicity determination. In: Lakkas TD (ed) Heavy metals in the environment, vol 2. CEP Consultants, Edinburg

Pueyo M, Mateu J, Rigol A, Vidal M, López-Sánchez JF, Rauret G (2008) Use of the modified BCR three-step sequential extraction procedure for the study of trace element dynamics in contaminated soils. Environ Pollut 152(2):330–341

Ščančar J, Milačič R, Horvat M (2000) Comparison of various digestion and extraction procedures in analysis of heavy metals in sediments. Water Air Soil Poll 118(1–2):87–99

Schaanning MT, Hylland K, Eriksen DØ, Bergan TD, Gunnarson JS, Skei J (1996) Interactions between eutrophication and contaminants. II. Mobilization and bioaccumulation of Hg and Cd from marine sediments. Mar Pollut Bull 33(1–6):71–79

Seidel H, Wennrich R, Hoffmann P, Löser C (2006) Effect of different types of elemental sulfur on bioleaching of heavy metals from contaminated sediments. Chemosphere 62(9):1444–1453

Shen F, Liao R, Ali A, Mahar A, Guo D, Li R, Zhang Z (2017) Spatial distribution and risk assessment of heavy metals in soil near a Pb/Zn smelter in Feng County, China. Ecotoxicol Environ Saf 139:254–262

Shi H, Sun Y, Zhao X, Qu B (2013) Influence on sorption property of Pb by fractal and site energy distribution about sediment of Yellow River. Procedia Environ Sci 18:464–471

Simpson SL, Apte SC, Batley GE (2000) Effect of short-term resuspension events on the oxidation of cadmium, lead, and zinc sulfide phases in anoxic estuarine sediments. Environ Sci Technol 34(21): 4533–4537

Singh KP, Mohan D, Singh VK, Malik A (2005) Studies on distribution and fractionation of heavy metals in Gomti river sediments—a tributary of the Ganges, India. J Hydrol 312(1–4):14–27

Stockdale A, Davison W, Zhang H (2009) Micro-scale biogeochemical heterogeneity in sediments: a review of available technology and observed evidence. Earth-Sci Rev 92(1–2):81–97

Tang W, Shan B, Zhang H, Zhang W, Zhao Y, Ding Y, Rong N, Zhu X (2014) Heavy metal contamination in the surface sediments of representative limnetic ecosystems in eastern China. Sci Rep 4:7152

Tang Q, Bao Y, He X, Fu B, Collins AL, Zhang X (2016) Flow regulation manipulates contemporary seasonal sedimentary dynamics in the reservoir fluctuation zone of the Three Gorges Reservoir, China. Sci Total Environ 548:410–420

Tankere-Muller S, Zhang H, Davison W, Finke N, Larsen O, Stahl H, Glud RN (2007) Fine scale remobilisation of Fe, Mn, Co, Ni, Cu and Cd in contaminated marine sediment. Mar Chem 106(1–2):192–207

Tsai LJ, Yu KC, Chen SF, Kung PY, Chang CY, Lin CH (2003) Partitioning variation of heavy metals in contaminated river sediment via bioleaching: effect of sulfur added to total solids ratio. Water Res 37(19):4623–4630

Ullman WJ, Aller RC (1982) Diffusion coefficients in nearshore marine sediments 1. Limnol Oceanogr 27(3):552–556

Vodyanitskii YN (2010) Iron hydroxides in soils: a review of publications. Eurasian Soil Sci 43(11):1244–1254

Wang S, Jia Y, Wang S, Wang X, Wang H, Zhao Z, Liu B (2010) Fractionation of heavy metals in shallow marine sediments from Jinzhou Bay, China. J Environ Sci 22(1):23–31

Wang J, Chen J, Guo J, Dai Z, Yang H, Song Y (2017a) Speciation and transformation of sulfur in freshwater sediments: a case study in Southwest China. Water Air Soil Pollut 228(10):392

Wang G, Zhang S, Xiao L, Zhong Q, Li L, Xu G, Deng O, Pu Y (2017b) Heavy metals in soils from a typical industrial area in Sichuan, China: spatial distribution, source identification, and ecological risk assessment. Environ Sci Pollut Res 24(20):16618–16630

Warnken KW, Davison W, Zhang H (2008) Interpretation of in situ speciation measurements of inorganic and organically complexed trace metals in freshwater by DGT. Environ Sci Technol 42(18): 6903–6909

Williams PN, Islam S, Islam R, Jahiruddin M, Adomako E, Soliaman ARM, Rahman GKMM, Lu Y, Deacon C, Zhu Y, Meharg AA (2009) Arsenic limits trace mineral nutrition (selenium, zinc, and nickel) in Bangladesh rice grain. Environ Sci Technol 43(21): 8430–8436

Wu Z, Wang S, Jiao L (2015) Geochemical behavior of metals–sulfide–phosphorus at SWI (sediment/water interface) assessed by DGT

(diffusive gradients in thin films) probes. J Geochem Explor 156: 145–152

Xu D, Gao B, Gao L, Zhou H, Zhao X, Yin S (2016) Characteristics of cadmium remobilization in tributary sediments in three gorges reservoir using chemical sequential extraction and DGT technology. Environ Pollut 218:1094–1101

Yan C, Zeng L, Che F, Yang F, Wang D, Luo Z, Wang Z, Wang X (2018) High-resolution characterization of arsenic mobility and its correlation to labile iron and manganese in sediments of a shallow eutrophic lake in China. J Soils Sediments 18(5):2093–2106

Yin H, Zhu J (2016) In situ remediation of metal contaminated lake sediment using naturally occurring, calcium-rich clay mineral-based low-cost amendment. Chem Eng J 285:112–120

Yin H, Fan C, Ding S, Zhang L, Zhong J (2008) Geochemistry of iron, sulfur and related heavy metals in metal-polluted Taihu Lake sediments. Pedosphere 18(5):564–573

Zhang H, Davison W (1995) Performance characteristics of diffusion gradients in thin films for the in situ measurement of trace metals in aqueous solution. Anal Chem 67(19):3391–3400

Zhang ZW, Zheng GD, Shozugawa K, Matsuo M, Zhao YD (2013) Iron and sulfur speciation in some sedimentary-transformation-type of lead–zinc deposits in West Kunlun lead–zinc ore deposit zone, Northwest China. J Radioanal Nucl Chem 297(1):83–90

Zhang C, Yu ZG, Zeng GM, Jiang M, Yang ZZ, Cui F, Zhu M, Shen L, Hu L (2014) Effects of sediment geochemical properties on heavy metal bioavailability. Environ Int 73:270–281

Zhang Z, Li J, Mamat Z, Ye Q (2016) Sources identification and pollution evaluation of heavy metals in the surface sediments of Bortala River, Northwest China. Ecotoxicol Environ Saf 126:94–101

Zhang T, Zeng X, Zhang H, Lin Q, Su S, Wang Y, Bai L (2018) Investigation of synthetic ferrihydrite transformation in soils using two-step sequential extraction and the diffusive gradients in thin films (DGT) technique. Geoderma. 321:90–99

Zhang T, Zeng X, Zhang H, Lin Q, Su S, Wang Y, Bai L, Wu C (2019) The effect of the ferrihydrite dissolution/transformation process on mobility of arsenic in soils: investigated by coupling a two-step sequential extraction with the diffusive gradient in the thin films (DGT) technique. Geoderma. 352:22–32

Zhu C, Liao S, Wang W, Zhang Y, Yang T, Fan H, Wen H (2018) Variations in Zn and S isotope chemistry of sedimentary sphalerite, Wusihe Zn-Pb deposit, Sichuan Province, China. Ore Geol Rev 95: 639–648